

Limit on the production of a low-mass vector boson in $e^+e^- \rightarrow U\gamma$, $U \rightarrow e^+e^-$ with the KLOE experiment

A. Anastasi^{e,d}, D. Babusci^d, G. Bencivenni^d, M. Berlowski^t, C. Bloise^d, F. Bossi^d, P. Branchini^q, A. Budano^{p,q}, L. Caldeira Balkeståhl^s, B. Cao^s, F. Ceradini^{p,q}, P. Ciambrone^d, F. Curciarello^{e,b,k}, E. Czerwiński^c, G. D'Agostini^{l,m}, E. Danè^d, V. De Leo^q, E. De Lucia^d, A. De Santis^d, P. De Simone^d, A. Di Cicco^{p,q}, A. Di Domenico^{l,m}, R. Di Salvo^o, D. Domenici^d, A. D'Uffizi^d, A. Fantini^{n,o}, G. Felici^d, S. Fiore^{r,m}, A. Gajos^c, P. Gauzzi^{l,m}, G. Giardina^{e,b}, S. Giovannella^d, E. Graziani^q, F. Happacher^d, L. Heijmanskjöld^s, W. Ikegami Andersson^s, T. Johansson^s, D. Kamińska^c, W. Krzemien^t, A. Kupsc^s, S. Loffredo^{p,q}, G. Mandaglio^{e,f}, M. Martini^{d,j}, M. Mascolo^d, R. Messi^{n,o}, S. Miscetti^d, G. Morello^d, D. Moricciani^o, P. Moskal^c, A. Palladino^{d,l,*}, M. Papenbrock^s, A. Passeri^q, V. Patera^{i,m}, E. Perez del Rio^d, A. Ranieri^a, P. Santangelo^d, I. Sarra^d, M. Schioppa^{g,h}, M. Silarski^d, F. Sirghi^d, L. Tortora^q, G. Venanzoni^{d,*}, W. Wislicki^t, M. Wolke^s

^aINFN Sezione di Bari, Bari, Italy.

^bINFN Sezione di Catania, Catania, Italy.

^cInstitute of Physics, Jagiellonian University, Cracow, Poland.

^dLaboratori Nazionali di Frascati dell'INFN, Frascati, Italy.

^eDipartimento di Fisica e Scienze della Terra dell'Università di Messina, Messina, Italy.

^fINFN Gruppo collegato di Messina, Messina, Italy.

^gDipartimento di Fisica dell'Università della Calabria, Rende, Italy.

^hINFN Gruppo collegato di Cosenza, Rende, Italy.

ⁱDipartimento di Scienze di Base ed Applicate per l'Ingegneria dell'Università "Sapienza", Roma, Italy.

^jDipartimento di Scienze e Tecnologie applicate, Università "Guglielmo Marconi", Roma, Italy.

^kNovosibirsk State University, 630090 Novosibirsk, Russia.

^lDipartimento di Fisica dell'Università "Sapienza", Roma, Italy.

^mINFN Sezione di Roma, Roma, Italy.

ⁿDipartimento di Fisica dell'Università "Tor Vergata", Roma, Italy.

^oINFN Sezione di Roma Tor Vergata, Roma, Italy.

^pDipartimento di Matematica e Fisica dell'Università "Roma Tre", Roma, Italy.

^qINFN Sezione di Roma Tre, Roma, Italy.

^rENEA UTTMAT-IRR, Casaccia R.C., Roma, Italy.

^sDepartment of Physics and Astronomy, Uppsala University, Uppsala, Sweden.

^tNational Centre for Nuclear Research, Warsaw, Poland.

Abstract

The existence of a new force beyond the Standard Model is compelling because it could explain several striking astrophysical observations which fail standard interpretations. We searched for the light vector mediator of this dark force, the U boson, with the KLOE detector at the DAΦNE e^+e^- collider. Using an integrated luminosity of 1.54 fb^{-1} , we studied the process $e^+e^- \rightarrow U\gamma$, with $U \rightarrow e^+e^-$, using radiative return to search for a resonant peak in the dielectron invariant-mass distribution. We did not find evidence for a signal, and set a 90% CL upper limit on the mixing strength between the Standard Model photon and the dark photon, ϵ^2 , at 10^{-6} – 10^{-4} in the 5–520 MeV/ c^2 mass range.

Keywords: dark matter, dark forces, dark photon, U boson, A'

1. Introduction

The Standard Model (SM) of particle physics has received further confirmation with the discovery of the Higgs boson [1–3], however, there are strong hints of physics it cannot explain, such as neutrino oscillations [4] and the measured anomalous magnetic moment of the muon [5]. Furthermore, the SM does not provide a dark matter (DM) candidate usually advocated

as an explanation of the numerous gravitational anomalies observed in the universe. Many extensions of the SM [7?–10] consider a Weakly Interacting Massive Particle (WIMP) as a viable DM candidate and assume that WIMPs are charged under a new kind of interaction. The mediator of the new force would be a gauge vector boson, the U boson, also referred to as a dark photon or A'. It would be produced during WIMP annihilations, have a mass less than two proton masses, and a leptonic decay channel in order to explain the astrophysical observations recently reported by many experiments [11–21].

In the minimal theoretical model, the U boson is the lightest particle of the dark sector and can couple to the ordinary

*Corresponding authors

Email addresses: palladin@bu.edu (A. Palladino), graziano.venanzoni@lnf.infn.it (G. Venanzoni)

¹Present address: Department of Physics, Boston University, Boston, USA

SM photon only through loops of heavy dark particles charged under both SM $U(1)_Y$ and dark $U(1)_D$ symmetries [22–26]. These higher-order interactions would open a so-called kinetic mixing portal described in the theory by the Lagrangian term $\mathcal{L}_{\text{mix}} = -\frac{\varepsilon}{2} F_{ij}^{\text{EW}} F_{\text{Dark}}^{ij}$, where F_{ij}^{EW} is the SM hypercharge gauge field tensor and F_{Dark}^{ij} is the dark field tensor. The ε parameter represents the mixing strength and is the ratio of the dark and electromagnetic coupling constants. In principle, the dark photon could be produced in any process in which a virtual or real photon is involved but the rate is suppressed due to the very small coupling ($\varepsilon < 10^{-2}$). In this respect, high-luminosity $O(\text{GeV})$ -energy e^+e^- colliders play a crucial role in dark photon searches [27–29].

We investigated the $e^+e^- \rightarrow U\gamma$ process by considering the U boson decaying into e^+e^- . At the level of coupling accessible by KLOE in this channel the U boson is expected to decay promptly leaving its signal as a resonant peak in the invariant-mass distribution of the lepton pair. The energy scan was performed by applying the radiative return method which consists of selecting the events in which either electron or positron emits an initial-state radiation (ISR) photon which carries away a part of the energy and effectively changes the amount of the energy available for U boson production. The selected initial- and final-state particles are the same as in the radiative Bhabha scattering process so we receive contributions from resonant s -channel, non-resonant t -channel U boson exchanges, and from s - t interference. The finite-width effects related to s -channel annihilation sub-processes, scattering t -channel and s - t interference are of order of Γ_U/m_U for the integrated cross section and can be neglected with respect to any potential resonance we would observe; $\Gamma_U \sim 10^{-7}$ – 10^{-2} MeV for the coupling strengths to which we are sensitive [30]. The non-resonant t -channel effects would not produce a peak in the invariant-mass distribution but could, in principle, appear in analyses of angular distributions or asymmetries. We are going to report exclusively on resonant s -channel U boson production.

Using a sample of KLOE data collected during 2004–2005, corresponding to an integrated luminosity of 1.54 fb^{-1} , we derived a new limit on the kinetic mixing parameter, ε^2 , approaching the dielectron mass threshold.

2. KLOE detector

The Frascati ϕ factory, DAΦNE, is an e^+e^- collider running mainly at a center-of-mass energy of 1.0195 GeV, the mass of the ϕ meson. Equal energy electron and positron beams collide at an angle of ~ 25 mrad, producing ϕ mesons nearly at rest.

The KLOE detector consists of a large cylindrical Drift Chamber (DC) [31] with a 25 cm internal radius, 2 m outer radius, and 3.3 m length, comprising $\sim 56,000$ wires for a total of about 12,000 drift cells. It is filled with a low- Z (90% helium, 10% isobutane) gas mixture and provides a momentum resolution of $\sigma_{p_\perp}/p_\perp \approx 0.4\%$. The DC is surrounded by a lead-scintillating fiber electromagnetic calorimeter (EMC) [32] composed of a cylindrical barrel and two end-caps providing 98% coverage of the total solid angle. Calorimeter modules are

read out at both ends by 4880 photomultiplier tubes, ultimately resulting in an energy resolution of $\sigma_E/E = 5.7\%/\sqrt{E(\text{GeV})}$ and a time resolution of $\sigma_t = 57 \text{ ps}/\sqrt{E(\text{GeV})} \oplus 100 \text{ ps}$. A superconducting coil around the EMC provides a 0.52 T field to measure the momentum of charged particles. A cross sectional diagram of the KLOE detector is shown in Figure 1.

The trigger [33] uses energy deposition in the calorimeter and drift chamber hit multiplicity. To minimize backgrounds the trigger system includes a second-level cosmic-ray muon veto based on energy deposition in the outermost layers of the calorimeter, followed by a software background filter based on the topology and multiplicity of energy clusters and drift chamber hits to reduce beam background. A downscaled sample is retained to evaluate the filter efficiency.

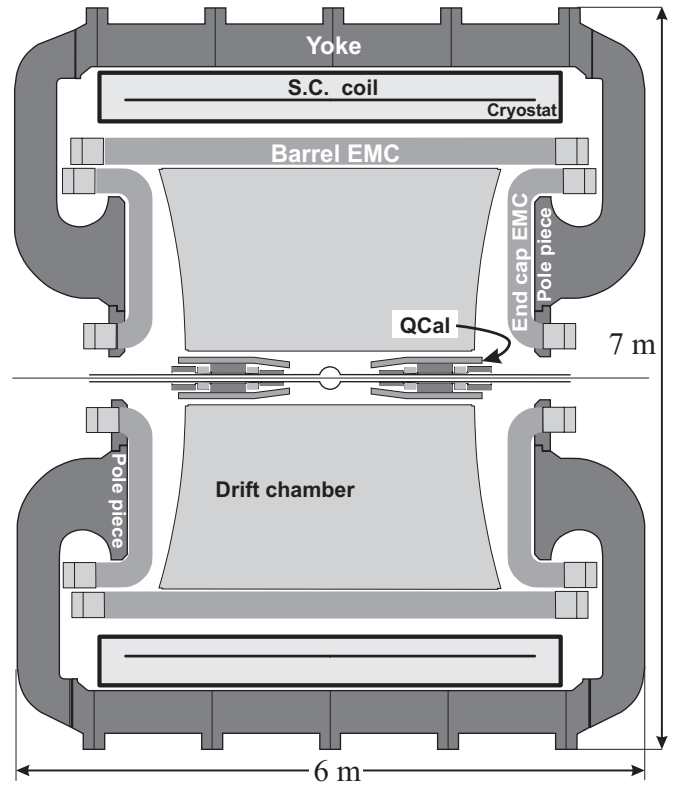


Figure 1: Cross section of the KLOE detector.

3. Event selection

Using 1.54 fb^{-1} of KLOE data we have searched for U boson production in the process $e^+e^- \rightarrow U\gamma$ followed by $U \rightarrow e^+e^-$. The center-of-mass energy of the collision depends on the amount of energy carried away by the initial-state radiation (ISR) photon. The irreducible background originates from the $e^+e^- \rightarrow e^+e^-\gamma$ radiative Bhabha scattering process, having the same three final-state particles. The reducible backgrounds consist of $e^+e^- \rightarrow \mu^+\mu^-\gamma$, $e^+e^- \rightarrow \pi^+\pi^-\gamma$, $e^+e^- \rightarrow \gamma\gamma$ (where one photon converts into an e^+e^- pair), and $e^+e^- \rightarrow \phi \rightarrow \rho\pi^0 \rightarrow \pi^+\pi^-\pi^0$, as well as other ϕ decays. The expected U boson signal would appear as a resonant peak in the invariant-mass distribution of the e^+e^- pair, m_{ee} . This search differs from

the previous KLOE searches [34–36] in its capability to probe the low mass region close to the dielectron mass threshold.

We selected events with three separate calorimeter energy deposits corresponding to two oppositely-charged lepton tracks and a photon. The final-state electron, positron, and photon were required to be emitted at large angle ($55^\circ < \theta < 125^\circ$) with respect to the beam axis, such that they are explicitly detected in the barrel of the calorimeter, see Figure 1. The large-angle selection greatly suppresses the t -channel contribution from the irreducible Bhabha-scattering background which is strongly peaked at small angle. Since we are interested mostly in the low invariant-mass region, we select only events with a hard photon, $E_\gamma > 305$ MeV, chosen to select a subsample of the events generated by our MC simulation. We required both lepton tracks to have a first DC hit within a radius of 50 cm from the beam axis and a point-of-closest-approach (PCA) to the beam axis within the fiducial cylinder, $\rho_{\text{PCA}} < 1$ cm and $-6 < z_{\text{PCA}} < 6$ cm, entirely contained within the vacuum pipe eliminating background events from photons converting on the vacuum wall. We eliminated tightly spiralling tracks by requiring either a large transverse or a large longitudinal momentum for each of the lepton tracks, $p_T > 160$ MeV/c or $p_z > 90$ MeV/c. We require that the total momentum of the charged tracks is $(|p_{e^+}| + |p_{e^-}|) > 150$ MeV/c to avoid the presence of poorly reconstructed tracks. A pseudo-likelihood discriminant was used to separate electrons from muons and pions [37]. A further discrimination from muons and pions was achieved using the M_{track} variable. M_{track} is the X mass for an $X^+X^-\gamma$ final state, computed using energy and momentum conservation, assuming $m_{X^+} = m_{X^-}$ [37]. In Figure 2 the M_{track} distribution is reported for measured data and for all the relevant MC simulated background components. Including the cut $M_{\text{track}} < 70$ MeV/c² we were left with 681,196 events at the end of the full analysis chain.

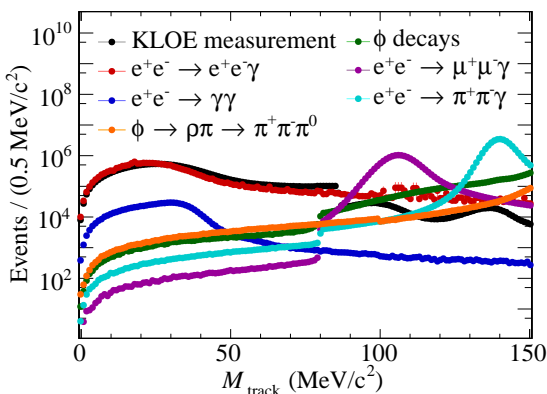


Figure 2: (color online) The track mass distribution before event selection for measurement and expected background simulations. Some of the simulations had a prescaling for $M_{\text{track}} < 80$ MeV/c², which has been accounted for in the background evaluation. The measurement data set was prescaled for $M_{\text{track}} > 85$ MeV/c². The track mass variable peaks at the mass of the charged track in the final state for events with two charged tracks and a photon. The selection region is $M_{\text{track}} < 70$ MeV/c².

4. Simulation and efficiencies

We used MC event generators interfaced with the full KLOE detector simulation, GEANFI [38], including detector resolutions and beam conditions on a run-by-run basis, to estimate the level of background contamination due to all of the processes listed in the previous section. Excluding the irreducible background from radiative Bhabha scattering events, the contamination from the sum of residual backgrounds after all analysis cuts is less than 1.5% in the whole m_{ee} range, and none of the background shapes are peaked, eliminating the possibility of a background mimicking the resonant U boson signal. The irreducible Bhabha scattering background was simulated using the BABAYAGA-NLO [39–42] event generator implemented within GEANFI (including the s -, t -, and s - t interference channels) and is shown in Figure 3 along with the measured data after subtracting the non-irreducible background components. No signal peak is observed.

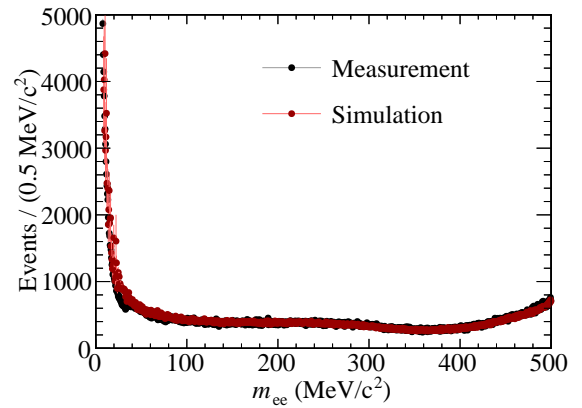


Figure 3: (color online) Dielectron invariant-mass distribution from measurement data with non-irreducible backgrounds subtracted compared to the BABAYAGA-NLO MC simulation.

In order to evaluate the U boson selection efficiency we used a modified version of the BABAYAGA-NLO event generator implemented within GEANFI, such that the radiative Bhabha scattering process was only allowed to proceed via the annihilation channel, in which the U boson resonance would occur. In order to create a large-statistics sample in our region of interest we restricted the BABAYAGA-NLO generated events to within $50^\circ < \theta_{e^+e^-}^{\text{MC}} < 130^\circ$ and $E_\gamma^{\text{MC}} > 300$ MeV. The generator-level efficiency due to this restriction was evaluated using a PHOKHARA MC simulation [43]. The total efficiency is evaluated as the product of the generator-level efficiency and the event-selection efficiency, containing the cuts in Section 3 conditioned to the generator-level restriction as well as the trigger efficiency, and is shown in Figure 4. The decrease in efficiency as $m_{ee} \rightarrow 2m_e$ comes from the requirement on the total momentum of the charged tracks.

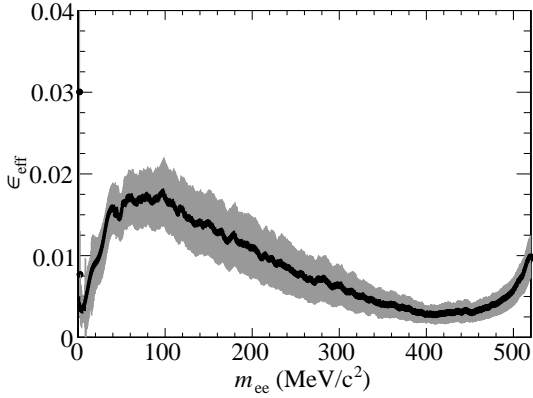


Figure 4: Smoothed distribution of the total efficiency defined as the product of the selection efficiency for the $e^+e^- \rightarrow U\gamma \rightarrow e^+e^-\gamma$ final state evaluated using the Babayaga-NLO event generator modified to allow only the s -channel process, and the generator-level efficiency evaluated from a PHOKHARA MC simulation.

5. Upper limit evaluation

We used the CL_S technique [44] to determine the limit on the number of signal U boson events, N_U , at 90% confidence level using the m_{ee} distribution. The invariant-mass resolution, $\sigma_{m_{ee}}$, is in the range $1.4 < \sigma_{m_{ee}} < 1.7 \text{ MeV}/c^2$. Chebyshev polynomials were fit to the measured data ($\pm 15\sigma_{m_{ee}}$), excluding the signal region of interest ($\pm 3\sigma_{m_{ee}}$). The polynomial with χ^2/N_{dof} closest to 1.0 was used as the background. A Breit-Wigner peak with a width of 1 keV smeared with the invariant-mass resolution was used as the signal. An example of one specific CL_S result is shown in Figure 5, yielding an upper limit of $N_U = 215$ U boson events at $m_U = 155.25 \text{ MeV}/c^2$ at the 90% confidence level. The χ^2/N_{dof} was 1.09 for this Chebyshev-polynomial sideband fit.

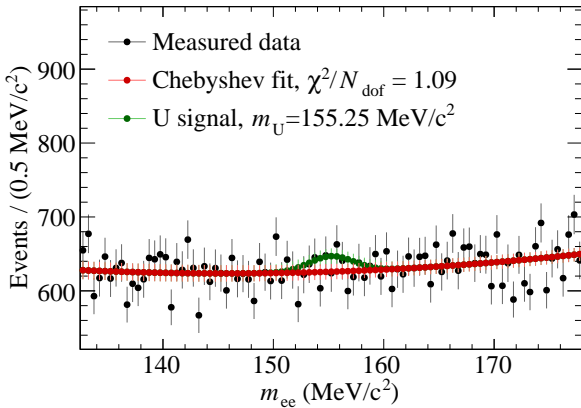


Figure 5: (color online) The CL_S result at 90% CL for $m_U = 155.25 \text{ MeV}/c^2$ showing the measured data, the Chebyshev-polynomial sideband fit, and the signal shape scaled to the CL_S result.

The upper limit at 90% confidence level on the number of U boson events, $\text{UL}(N_U)$, can be translated into a limit on the

cross section,

$$\text{UL}[\sigma(e^+e^- \rightarrow U\gamma, U \rightarrow e^+e^-)] = \frac{\text{UL}(N_U)}{L \epsilon_{\text{eff}}}, \quad (1)$$

where L is the luminosity and ϵ_{eff} is the total selection efficiency. The limit is shown in Figure 6.

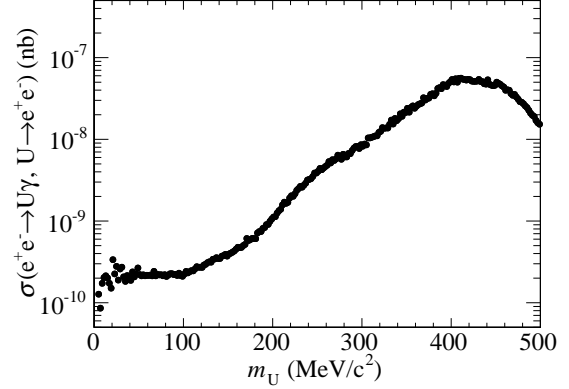


Figure 6: Upper limit on the cross section $\sigma(e^+e^- \rightarrow U\gamma, U \rightarrow e^+e^-)$.

We then translated the limit on N_U to a 90% confidence level limit on the kinetic mixing parameter as a function of m_{ee} as in [36],

$$\varepsilon^2(m_{ee}) = \frac{N_U(m_{ee})}{\epsilon_{\text{eff}}(m_{ee})} \frac{1}{H(m_{ee}) I(m_{ee}) L}, \quad (2)$$

where the radiator function $H(m_{ee})$ was extracted from

$$d\sigma_{ee\gamma}/dm_{ee} = H(m_{ee}, s, \cos(\theta_\gamma)) \cdot \sigma_{ee}^{\text{QED}}(m_{ee})$$

using the PHOKHARA MC simulation [43] to determine the radiative differential cross section, $I(m_{ee})$ is the integral of the cross section $\sigma(e^+e^- \rightarrow U \rightarrow e^+e^-)$, $L = 1.54 \text{ fb}^{-1}$ is the integrated luminosity, and $\epsilon_{\text{eff}}(m_{ee})$ is the total efficiency described in Section 4. Our limit is shown in Figure 7 along with the indirect limits from the measurements of $(g-2)_e$ and $(g-2)_\mu$ at 5σ shown with dashed curves. Limits from the following direct searches are shown with shaded regions and solid curves: E141 [45], E774 [45], KLOE($\phi \rightarrow \eta U, U \rightarrow e^+e^-$) [34, 35], Apex [46], WASA [47], HADES [48], A1 [49], KLOE($e^+e^- \rightarrow U\gamma, U \rightarrow \mu^+\mu^-$) [36], BaBar [50], and NA48/2 [51].

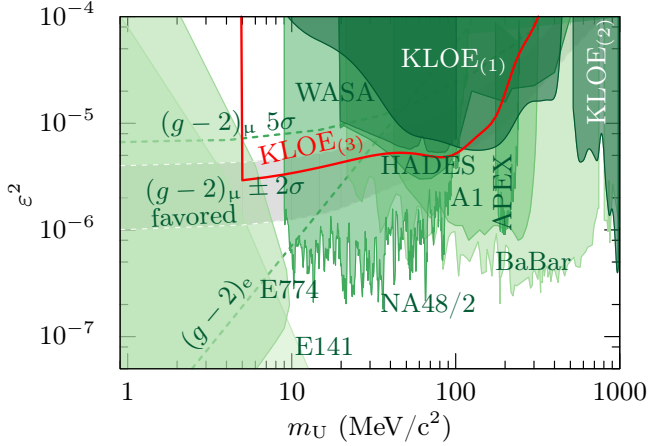


Figure 7: (color online) Exclusion limits on the kinetic mixing parameter squared, ϵ^2 , as a function of the U boson mass. The red curve labeled $\text{KLOE}_{(3)}$ is the result of this article while the curves labeled $\text{KLOE}_{(1)}$ and $\text{KLOE}_{(2)}$ indicate the previous KLOE results. Also shown are the exclusion limits provided by E141, E774, Apex, WASA, HADES, A1, BaBar, and NA48/2. The gray band delimited by the dashed white lines indicates the mixing level and m_U parameter space that could explain the discrepancy observed between the measurement and SM calculation of the muon $(g-2)_\mu$.

6. Systematic uncertainties

The background was determined by Chebyshev-polynomial sideband fits. The parameters of the polynomials were then varied within 1σ to determine the maximum variation of the polynomial shape. The uncertainty of each bin was set to the extent of that variation evaluated at the bin center. An example of the error bars on the Chebyshev-polynomial sideband fits can be seen in Figure 5. These bin uncertainties were taken into account in the CL_S procedure when determining $N_{\text{CL}_S}(m_{ee})$. Since the irreducible background is smooth for each fit range, we assume the Chebyshev polynomials sufficiently represent the background with negligible systematic uncertainty. Any uncertainty in the shape of the smeared resonant peak was also taken to be negligible.

The efficiency of the $e^+e^- \rightarrow e^+e^-\gamma$ event selection was determined by taking the ratio of the set of simulated events that passed the selection criteria to the total simulated sample. We apply a 0.1% systematic uncertainty due to the BABAYAGANLO event generator [39–42], a 0.1% systematic uncertainty for the trigger, and a 0.1% systematic uncertainty for the software background filter. All together the uncertainty on the selection efficiency is dominated by the statistical uncertainty on the selected sample. A PHOKHARA MC simulation [43] was performed to evaluate the generator-level efficiency due to the restriction $E_\gamma^{\text{MC}} > 300 \text{ MeV}$ and $50^\circ < \theta_{e^+e^-}^{\text{MC}} < 130^\circ$. The selection efficiency and the generator-level efficiency are combined to give the total efficiency, $\epsilon_{\text{eff}}(m_{ee})$. The uncertainty is given as the error band in Figure 4, again dominated by the statistical uncertainties in the simulated data set.

There are two effects that contribute to the uncertainty in the radiator function, $H(m_{ee})$. First, since the value of $H(m_{ee})$ is taken from simulated data, we must take into account the statis-

tical uncertainty on those values. Second, we assume a uniform 0.5% systematic uncertainty in the calculation of $H(m_{ee})$, as quoted in [43, 52–54]. The uncertainty in the integrated luminosity is 0.3% [37]. The uncertainties on $H(m_{ee})$, $\epsilon_{\text{eff}}(m_{ee})$, and L , propagate to the systematic uncertainty on $\epsilon^2(m_{ee})$ via (2). A summary of systematic uncertainties is presented in Table 1.

Table 1: Summary of systematic uncertainties. The uncertainties on the efficiency, radiator function, and cross-section integral vary as a function of m_{ee} . The numbers quoted here correspond to the largest estimate within our m_{ee} range.

Systematic source	Relative uncertainty
Background (sideband fit)	negl.
$\epsilon_{\text{eff}}(m_{ee})$	2%
MC generator, 0.1%	
Trigger, 0.1%	
Software background filter, 0.1%	
Event selection, 2%	
$H(m_{ee})$	0.5%
$I(m_{ee})$	negl.
L	0.3%

7. Conclusions

We performed a search for a dark gauge U boson in the process $e^+e^- \rightarrow U\gamma$ with $U \rightarrow e^+e^-$ using the radiative return method and 1.54 fb^{-1} of KLOE data collected in 2004–2005. We found no evidence for a U boson resonant peak and set a 90% CL upper limit on the kinetic mixing parameter, ϵ^2 , at 10^{-6} – 10^{-4} in the U-boson mass range 5–520 MeV/c^2 . This limit partly excludes some of the remaining parameter space in the low dielectron mass region allowed by the discrepancy between the observed and predicted $(g-2)_\mu$.

8. Acknowledgments

We warmly thank our former KLOE colleagues for the access to the data collected during the KLOE data taking campaign. We thank the DAΦNE team for their efforts in maintaining low background running conditions and their collaboration during all data taking. We want to thank our technical staff: G.F. Fortugno and F. Sborzacchi for their dedication in ensuring efficient operation of the KLOE computing facilities; M. Anelli for his continuous attention to the gas system and detector safety; A. Balla, M. Gatta, G. Corradi and G. Papalino for electronics maintenance; M. Santoni, G. Paoluzzi and R. Rosellini for general detector support; C. Piscitelli for his help during major maintenance periods. This work was supported in part by the EU Integrated Infrastructure Initiative Hadron Physics Project under contract number RII3-CT- 2004-506078; by the European Commission under the 7th Framework Programme through the ‘Research Infrastructures’ action of the ‘Capacities’ Programme, Call: FP7-INFRASTRUCTURES-2008-1, Grant

Agreement No. 227431; by the Polish National Science Centre through the Grants No. DEC-2011/03/N/ST2/02641, 2011/03/N/ST2/02652, 2013/08/M/ST2/00323, 2013/11/B/ST2/04245, 2014/14/E/ST2/00262, and by the Foundation for Polish Science through the MPD programme.

In addition, we would like to thank the BABAYAGA authors, C.M. Carloni Calame, G. Montagna, O. Nicrosini, and F. Piccinini, for numerous useful discussions and help while modifying their code for our purpose.

References

- [1] ATLAS Collaboration, Phys. Lett. B 716 (2012) 1–29.
- [2] CMS Collaboration, Phys. Lett. B 716 (2012) 30–61.
- [3] CMS Collaboration, J. High Energy Phys. 06 (2013) 081.
- [4] K. Olive, et al., Review of Particle Physics, Chapter 14: Neutrino Mass, Mixing, and Oscillations, Chin.Phys. C38 (2014) 090001. doi: 10.1088/1674-1137/38/9/090001.
- [5] J. Miller, et al., Ann. Rev. Nucl. and Part. Sci. 62 (2012) 237.
- [6] M. Pospelov, A. Ritz, M. B. Voloshin, Phys. Lett. B 662 (2008) 53.
- [7] N. Arkani-Hamed, et al., Phys. Rev. D 79 (2009) 015014.
- [8] D. S. M. Alves, et al., Phys. Lett. B 692 (2010) 323.
- [9] M. Pospelov, A. Ritz, Phys. Lett. B 671 (2009) 391.
- [10] N. Arkani-Hamed, N. Weiner, JHEP 0812 (2008) 104.
- [11] P. Jean, et al., Astron. Astrophys. 407 (2003) L55.
- [12] O. Adriani, et al., Nature 458 (2009) 607.
- [13] M. Aguilar et al., AMS Collaboration, Phys. Rev. Lett. 110 (2013) 141102.
- [14] J. Chang, et al., Nature 456 (2008) 362.
- [15] A. A. Abdo, et al., Phys. Rev. Lett. 102 (2009) 181101.
- [16] F. Aharonian et al., HESS Collaboration, Phys. Rev. Lett. 101 (2008) 261104.
- [17] F. Aharonian et al., HESS Collaboration, Astron. Astrophys. 508 (2009) 561.
- [18] R. Bernabei, et al., Int. J. Mod. Phys. D 13 (2004) 2127.
- [19] R. Bernabei, et al., Eur. Phys. J. C 56 (2008) 333.
- [20] C. E. Aalseth et al., CoGeNT Collaboration, Phys. Rev. Lett. 106 (2011) 131301.
- [21] C. E. Aalseth et al., CoGeNT Collaboration, Phys. Rev. Lett. 107 (2011) 141301.
- [22] B. Holdom, Phys. Lett. B 166 (1985) 196.
- [23] C. Boehm, P. Fayet, Nucl. Phys. B 683 (2004) 219.
- [24] N. Borodatchenkova, D. Choudhury, M. Drees, Phys. Rev. Lett. 96 (2006) 141802.
- [25] P. Fayet, Phys. Rev. D 75 (2007) 115017.
- [26] Y. Mambrini, J. Cosmol. Astropart. Phys. 1009 (2010) 022.
- [27] R. Essig, P. Schuster, N. Toro, Phys. Rev. D 80 (2009) 015003.
- [28] B. Batell, M. Pospelov, A. Ritz, Phys. Rev. D 79 (2009) 115008.
- [29] M. Reece, L. Wang, JHEP 0907 (2009) 051.
- [30] L. Barzè, et al., The European Physical Journal C 71 (6). doi:10.1140/epjc/s10052-011-1680-8, [link].
URL <http://dx.doi.org/10.1140/epjc/s10052-011-1680-8>
- [31] M. Adinolfi, et al., Nucl. Instr. Meth. A 488 (2002) 51.
- [32] M. Adinolfi, et al., Nucl. Instr. Meth. A 482 (2002) 364.
- [33] M. Adolfini et al., Nucl. Instrum. & Methods 492 (2002) 134.
- [34] F. Archilli et al., KLOE-2 Collaboration, Phys. Lett. B 706 (2012) 251–255.
- [35] D. Babusci et al., KLOE-2 Collaboration, Phys. Lett. B 720 (2013) 111–115.
- [36] D. Babusci et al., KLOE-2 Collaboration, Phys. Lett. B 736 (2014) 459–464.
- [37] A. Denig, et al., KLOE note 192[link].
URL www.lnf.infn.it/kloe/pub/knote/kn192.ps
- [38] F. Ambrosino et al., KLOE-2 Collaboration, Nucl. Instrum. & Methods 534 (2004) 403.
- [39] L. Barzè, et al., Eur. Phys. J. C 71 (2011) 1680.
- [40] G. Balossini, et al., Nucl. Phys. B 758 (2006) 227.
- [41] C. M. C. Calame, Phys. Lett. B 520 (2001) 16.
- [42] C. M. C. Calame, et al., Nucl. Phys. B 584 (2000) 459.
- [43] H. Czyż, et al., Eur. Phys. J. C 39 (2005) 411.
- [44] G. C. Feldman, R. D. Cousins, Phys. Rev. D 57 (1998) 3873.
- [45] J. D. Bjorken, et al., Phys. Rev. D 80 (2009) 075018. [link].
URL <http://arxiv.org/abs/0906.0508>
- [46] S. Abrahamyan et al., APEX Collaboration, Phys. Rev. Lett. 107 (2011) 191804.
- [47] P. Adlarson et al., WASA-at-COSY Collaboration, Phys. Lett. B 726 (2013) 187.
- [48] G. Agakishiev et al., HADES Collaboration, Phys. Lett. B 731 (2014) 265–271.
- [49] H. Merkel et al., A1 Collaboration, Phys. Rev. Lett. 112 (2014) 221802.
- [50] J.P. Lees et al., BaBar Collaboration, Phys. Rev. Lett. 113 (2014) 201801. doi:10.1103/PhysRevLett.113.201801, [link].
URL <http://link.aps.org/doi/10.1103/PhysRevLett.113.201801>
- [51] J.R. Batley et al., NA48/2 Collaboration, Phys. Lett. B 746 (2015) 178–185.
- [52] G. Rodrigo, H. Czyż, J. H. Kühn, M. Szopa, Eur. Phys. J. C 24 (2002) 71.
- [53] H. Czyż, A. Grzelinska, J. H. Kühn, G. Rodrigo, Eur. Phys. J. C 27 (2003) 563.
- [54] H. Czyż, A. Grzelinska, J. H. Kühn, G. Rodrigo, Eur. Phys. J. C 33 (2004) 333.